The unfavorable lipid environment reduced caveolin-1 expression in apical membranes from human preeclamptic placentas

Lorena Levi [a], Mauricio Castro-Parodi [a], Nora Martínez [b], Lidia L. Piehl [c], Emilio Rubín De Celis [c], Vanesa Herlax [d], Sabina Mate [d], Mariana Farina [e], Alicia E. Damiano [a,b,*]

[a] Departamento de Ciencias Biológicas, Facultad de Farmacia y Bioquímica, Universidad de Buenos Aires, Buenos Aires, Argentina
[b] Laboratorio de Biología de la Reproducción, Instituto de Fisiología y Biofísica Bernardo Houssay (IFIBIO)- CONICET- Facultad de Medicina, Universidad de Buenos Aires, Buenos Aires, Argentina
[c] Departamento de Fisicomatemática, Facultad de Farmacia y Bioquímica, Universidad de Buenos Aires, Buenos Aires, Argentina
[d] Instituto de Investigaciones Bioquímicas de La Plata (INIBIOLP), CCT-La Plata, CONICET, Facultad de Ciencias Médicas, Universidad Nacional de La Plata, Buenos Aires, Argentina
[e] Laboratorio de Fisiopatología Placentaria, CEFyBO, Facultad de Medicina, Universidad de Buenos Aires, Buenos Aires, Argentina

ARTICLE INFO

ABSTRACT

Syncytialization process is associated with a reduction in the number of caveolas, and a decreased of caveolin-1 (Cav-1). Differentiation of syncytiotrophoblast affects the membranes phospholipid composition. Thus, disturbances in these processes are related to pathological conditions such as preeclampsia.

Objective: To analyse the lipid composition of the apical (MVM) and the basal (BM) membranes of syncytiotrophoblast and its relationship with Cav-1 expression in normal and preeclamptic placentas. Molecular expression of Cav-1 was determined in MVM and BM from normal and preeclamptic placentas and in detergent-resistant membranes (DRMs). Phospholipids were analyzed by thin layer chromatography. Cholesterol was also determined by enzymatic assay. Membrane fluidity was evaluated by electron paramagnetic resonance. Sphingomyelin (SM) molecular species were analyzed and quantified by gas-liquid chromatography and mass spectrometry.

Cav-1 was significantly reduced in MVM from preeclamptic placentas. Regarding Cav-1 localization, it was barely detectable in syncytiotrophoblast but it was present in the endothelium. Western blots also showed a significantly decrease of Cav-1 in the apical DRMs from preeclamptic placentas. Lipid analysis showed an increase SM in MVM from preeclamptic placentas without changes in cholesterol. Preeclamptic MVM fluidity decreased significantly and we found an increase in C18:1 fatty acids of SM.

We concluded that preeclamptic-MVMs are more rigid than normal ones, possible due to an increment on SM. Moreover, the increase of long and unsaturated SM molecular specie found in these vesicles may disrupt the ability of SM to assemble into lipid rafts in the luminal leaflet of the bilayer, creating an unfavorable environment for Cav-1.

© 2016 Elsevier B.V. All rights reserved.

1. Introduction

Differentiation of human trophoblast cells involves a process that culminates in the formation of terminally multinucleated syncytiotrophoblast cells. Resulting from the fusion with the underlying cytotrophoblast cells, it forms a polarized syncytium with its apical brush border membrane (MVM) facing the maternal circulation and the smooth basal membrane (BM) facing the fetal circulation. Although, the mechanisms controlling syncytiotrophoblast formation are undefined, it is well established that the fusion of cytotrophoblast is essential for the maintenance of a successful pregnancy [1].

Emerging evidence shows that differentiation of syncytiotrophoblast affects the phospholipid composition of plasma membrane. It was found that the composition, structure and functions of these membrane lipid bilayers are modified with gestational progress in order to meet the metabolic needs of the growing fetus [2,3]. In addition, in pathological conditions such as preeclampsia, some authors have found alterations in membrane lipid composition of syncytiotrophoblast [4,5] and an abnormal expression of transport proteins [6–9] impairing placental functions.

Lipids are the principal components of biological membranes and play essential roles in cellular function regulating important processes such as proliferation, apoptosis, metabolism and cell migration [10].

Thus, a disturbance in the lipid signaling pathways may contribute to the progression of several diseases [11,12].

Recently, Korkes and co-workers demonstrated that lipids found in plasma and placental tissue from pregnant women with preeclampsia, differ from those expressed in healthy pregnancies [4]. In addition, other authors reported that syncytiotrophoblast microvesicles (STBMs) from preeclamptic women have a different pattern and distinct concentrations of some lipid species compared to STBMs from control group [5]. However, up to now, it is unknown if these changes are related to the pathogenesis of preeclampsia.

It is well-established that sphingomyelin (SM) and cholesterol (Cho) constitute various types of microdomains in plasma membranes such as caveolas [12]. Caveolas are plasma membrane invaginations, 50–100 nm in diameter, important in endocytosis, lipid trafficking, and signal transduction [13,14]. Originally discovered in the endothelium [15], caveolas have now been identified in many cell types including epithelium, adipocytes, fibroblasts, and smooth, skeletal, and cardiac muscle cells. Caveolin proteins are the major structural component of caveolas. Three caveolin isoforms have been described in mammalian cells: caveolin-1 (Cav-1), caveolin-2 (Cav-2), and caveolin-3 (Cav-3). Cav-1 and Cav-2 are co-expressed in most cell types and are required for the formation of caveolas, while Cav-3 is a muscle-specific protein, predominantly expressed in skeletal and cardiac muscle [16]. Caveolins have been implicated in the pathogenesis of various organ injuries and in conditions such as ischemia, in which a mismatch occurs between energy production and utilization. Such conditions are associated with altered expression of caveolas or redistribution of caveolin; for instance, hypoxic injury imposed on renal proximal tubules causes Cav-1 release, accompanied with caveolas disruption, and Cav-1 appearing within the extracellular space was largely in the denatured form [17].

In human placenta, Cav-1 is strongly expressed in endothelial cells, with lower levels in cytotrophoblasts, mesenchymal cells, and syncytiotrophoblast [18–21].

Unlike the situation reported for other differentiated cells, syncytialization process was associated with a mark reduction in the number of caveolas, and a decreased expression of Cav-1 [22]. Although the reduction in Cav-1 as trophoblasts syncytialise may simply be a feature of the loss of lateral cell membranes following cell fusion, it is unknown whether disturbances in this process may alter the expression in Cav-1.

Recently, Smith-Jackson and coworkers have described a decreased expression of Cav-1 in preeclamptic placentas [23]. However, whether changes in the membrane lipid composition of syncytiotrophoblast may affect the expression of Cav-1 was not investigated.

In the present work, we examined the lipid composition of the apical and the basal membranes of syncytiotrophoblast and its relationship with the expression of Cav-1 in normal and preeclamptic placentas.

2. Materials and methods

2.1. Tissue collection

This study was approved by the local ethics committees of the "Hospital Nacional Dr. Prof. Alejandro Posadas", Buenos Aires, Argentina, and written consent was obtained from patients before the collection of samples.

Full-term normal ($n = 32$) and severe preeclamptic ($n = 30$) placental tissues were obtained after cesarean section (Table 1).

Severe preeclampsia was defined as systolic blood pressure ≥ 170 mm Hg and/or diastolic pressure ≥ 110 mm Hg, with proteinuria ≥0.3 g/d or 2 pluses on urine dipstick after the 20th week of gestation in a previously normotensive patient. The preeclamptic women were identified as late-onset of preeclampsia.

Table 1
Clinical characteristics of severe preeclamptic and normotensive woman. Preeclamptic was defined as systolic blood pressure ≥ 160 mm Hg and/or diastolic pressure ≥ 110 mm Hg, with proteinuria ≥0.3 g/day.
Data are the means ± SD. Student's t-test was performed on the data.

	Term Control	Severe Preeclampsia
Number of pregnant women	32	30
Maternal age, yr	25.1 ± 4.3	26.3 ± 5.2
Gestational age, wks from LMP	38.8 ± 1.7	35.7 ± 2.6
Body Mass index (BM), kg/m^2	25 ± 3	24 ± 4
Proteinuria	Negative	+++
Mean blood pressure, mm Hg		
Systolic	111.0 ± 3.2[*]	160.3 ± 3.5[*]
Diastolic	63.9 ± 2.1[**]	113.0 ± 2.3[**]
Birth weight, g	3290 ± 513	2630 ± 1081

Values are means ± standard deviation.
LMP: last menstrual period.
 [*] $P < 0.01$.
 [**] $P < 0.01$.

2.2. RT-PCR Assay

Several placental cotyledons were removed from underlying fibrous elements and rinsed thoroughly in 0.9% NaCl at 4 °C. Soft villous material from the maternal surface enriched in trophoblast cells was cut away from connective tissue and vessels until approximately 1 g were collected. The tissue was rinsed again in order to remove most of the blood cells and then homogenized on ice for 30 s by using an Ultra-Turrax T25 blender at maximum speed. Total RNA from trophoblast cells was isolated by using an SV Total RNA isolation system (Promega Co., USA). Reverse transcription was performed for 60 min on 5 μg of total RNA by using moloney murine leukemia virus reverse transcriptase, oligo (dT)15 primer and 400 μM of each deoxyribonucleotide triphosphate (dNTP) at 42 °C. PCR (30 cycles) at 94 °C for 60 s, at 58 °C for 60 s and at 72 °C for 60 s, followed by a final extension of 10 min at 72 °C, was carried out by using 5 μM of a specific oligonucleotide primers for human Cav-1. These primers amplified a 434-bp region of human Cav-1 including nucleotides 313 through 747 (sense 5′-TCTC TACACCGTTCCCATCC-3′ and antisense 5′-CACAGACGGTGTGGACGT AG-3′). These primers were designed using http://www-genome.wi. mit.edu/cgi-bin/primer/primer3_www.cgi on the bases of Gene Bank sequences (accession number: NM_001753).

Control experiments were performed without the addition of reverse transcriptase to evaluate the absence of genomic DNA amplification.

2.3. Apical (MVM) and basal (BM) membrane vesicles isolation

Human placenta villi from normal term and preeclamptic placentas were processed according to the method previously described [24]. Briefly, human chorionic villi were fragmented, and washed with unbuffered 150 mM NaCl. The tissue was then shaken for 1 h with 1.5 volumes of HES buffer (10 mM HEPES-KOH, 0.1 mM EGTA, 250 mM sucrose) pH 7.4, with protease inhibitors (0.2 mM PMSF, 25 μg/mL p-aminobenzamidine, 20 μg/mL aprotinin, 10 μg/mL leupeptin, 10 μg/mL pepstatin), followed by filtration and centrifugation at 3100 g for 10 min. The supernatant was then further centrifuged 10 min at 11,000 g and the resulting supernatant centrifuged 70 min at 16,000 g.

The pellet was then resuspended in HES buffer containing 10 mM MgCl$_2$ to selectively precipitate non-apical membranes. The suspension was then incubated 10 min with constant stirring, after which it was centrifuged 30 min at 5000 g. The basal membrane-enriched pellet was redissolved in HES buffer containing protease inhibitors, and stored at −80 °C. Finally, the supernatant was centrifuged 70 min at 16,000 g and the apical membrane-enriched pellet was resuspended in HES

buffer containing proteases inhibitors, and stored at −80 °C until assayed for biochemical markers. Alkaline phosphatase and adenylate cyclase activities (as markers for MVM and BM, respectively) were determined in the each membrane suspension. Enrichment of the membranes isolated was <20-fold for MVM and <11-fold for BM).

2.4. Western blot

For immunoblotting studies, 10–20 μg of membrane fraction proteins was dissolved in Laemmli loading buffer (4% sodium dodecyl sulphate, 0.125 M Tris-HCl pH 6.8, 0.2 M dithiothreitol, 0.02% bromophenol blue, 20% glycerol), heated to 90 °C for 2 min, resolved on 15% polyacrylamide gel and electrotransferred onto nitrocellulose membranes (Hybond ECL, Amersham Pharmacia Biotech Ltd., UK). Membranes were blocked with 1 (w/v) bovine serum albumin in TBS at room temperature for 30 min and incubated overnight with a rabbit polyclonal primary antibody (Santa Cruz Biotechnology Inc., USA) against human Cav-1 diluted 1:1000. Membranes were washed with TBS-Tween 0.1%, and then with a goat anti-rabbit immunoglobulin G ([IgG] Jackson ImmunoResearch Laboratories, Inc. West Grove, PA, USA; 1:10,000) conjugated to peroxidase. Immunoreactivity was detected using the Enhanced Chemiluminescence (ECL) Western Blotting Analysis System (ECL plus, Amersham Pharmacia Biotech Ltd., Pittsburgh, PA USA) according to the manufacturer's instructions.

The densitometry of the bands was quantified by the ImageJ 1.45s software package (Bethesda, MD, USA).

To confirm equal loading, each membrane was stripped and analyzed for β-actin protein expression, demonstrating that the band intensities did not present significant changes between the samples studied.

2.5. Immunohistochemistry

Human villous tissue from normal and preeclamptic placentas were cut into small pieces, fixed overnight in 10% formaldehyde - 0.1 M sodium phosphate buffer (PBS), pH 7.4, dehydrated, and embedded in paraffin. Paraffin sections (4 μm) were cut and mounted on 2% silanized slices, dried, dewaxed and rehydrated. Tissue slices were incubated in 3% H_2O_2/methanol for 5 min to block endogenous peroxidase, and washed three times in 10 mM PBS, pH 7.4, for 5 min. All subsequent steps were carried out in a humidified chamber. Non-specific binding sites were blocked by incubation at room temperature in blocking reagent (DAKO LSAB kit, Dako Corp., USA) for 30 min. Sections were incubated overnight with anti Cav-1 antibody at a dilution of 1:50. Sections were then washed with 0.05 M PBS for 5 min, incubated for 10 min in prediluted link antibody, washed again in PBS buffer and incubated for 30 min in a solution of streptavidin-conjugated horse-radish peroxidase in PBS. Color development of the antibody labeling was achieved under microscopic control by incubating slices with the substrate DAB/NiCl$_2$ (3,3′-diaminobenzidine/nickel chloride) and 0.3% hydrogen peroxide in distilled water. Counterstain by hematoxylin was performed. Non-immune mouse serum without primary antibody was used as a negative control.

2.6. Isolation of detergent-resistant membranes (DRMs) by sucrose gradient centrifugation

DRMs were prepared from MVM and BM vesicles obtained from preeclamptic and normal human placental syncytiotrophoblast following a previously detailed protocol [25] introducing minor modifications. Briefly, 1.5 mg of protein of each membranes were incubated at 4 °C during 30 min with TNE buffer (10 mM Tris, 200 mM NaCl, 1 mM EDTA, pH 7.4) containing Triton X-100, so that the final volume was 1 mL and the final detergent concentration 16 mM. Samples were dispersed by 10 passages through a 21-gauge needle. After incubation, the lysate was diluted with an equal volume of 80% (v/v) sucrose solution in TNE buffer containing 0.3 M Na$_2$CO$_3$. One milliliter of this suspension was overlayered by 2.3 mL of 35% sucrose, followed by 1 ml of a 5% sucrose, both solution prepared in TNE buffer. The samples were centrifuged at 190,000 g in a Beckman SW60 Ti rotor at 4 °C for 18 h. After ultracentrifugation, one fraction of 0.33 mL and four fractions of 1 mL were collected from the top of the tube and saved for subsequent characterization. All fractions were stored frozen at 20 °C for further analysis.

2.7. Protein detection in sucrose density gradient fractions

Sucrose gradient fractions of MVM and BM of syncytiotrophoblast from preeclamptic and normal placentas were subjected to SDS–PAGE 5%–20% (w/v) gradient polyacrylamide gels for Western blot analysis.

Prior to perform the electrophoresis, fractions were dialysed against TNE buffer overnight so as to eliminate sucrose. Then samples were concentrated to dryness by speed-vac. Finally, the precipitated were diluted in 30 μL of SDS-PAGE loading buffer.

After proteins were separated by SDS-PAGE 5–20%, gels were transferred to nitrocellulose membrane. After blocking blots were incubated with a solution containing a polyclonal anti-Cav-1 (Santa Cruz Biotechnology, Inc.; 1:1000) and revealed as we have described.

## 2.8. Lipid analysis

2.8.1. Major lipid classes

Total lipids from the purified MVM and BM vesicles were extracted according to the method of Bligh and Dyer [26]. Total phospholipid amount was determined by the method of Fiske and Subarrow [27] and Cholesterol content was measured by an enzymatic method with the commercial kit (Colestat®, Wiener Laboratory, Rosario, Argentina).

Individual phospholipids were separated from total lipid extracts by thin-layer chromatography (TLC) on high-performance TLC plates (Merck, Darmstadt, Germany) in order to determine and quantified the major phospholipid classes. The extracts were dissolved in chloroform, dried under nitrogen stream and applied to silica gel G precoated TLC plates (0.25 mm thick) and submitted to two-solvent, one-dimensional thin-layer chromatography. Solvents I and II were 40:10:10:1 (v/v) and 120:46:19:3 (v/v) chloroform:methanol:acetic acid:water, respectively. For the quantification of phospholipids, specific areas of the TLC plates were identified by comparison with commercial standards, scraped off and digested with 70% perchloric acid in the presence of ammonium molybdate (0.5%), for 2 h in a heating block at 180 °C. The resulting inorganic phosphate was assayed with a Fiske–Subbarow reagent [27].

2.8.2. Sphingomyelin species of MVM-vesicles from normal and preeclamptic placentas

Total lipids were extracted using the modified Bligh and Dyer's method described by Baig et al. [5]. Briefly, 750 μL of ice cold chloroform:methanol (1:2, v/v) was added to MVM-vesicles resuspended in 100 μL of PBS. The mixture was vortexed vigorously for 1 min. After shaking at 200 g at 4 °C for 1 h, 250 μL ice cold chloroform and 350 μL of ice cold water was added to the samples. The samples were then subjected to another 1 min vortexing. The phases were separated by centrifugation at 11,000 g for 2 min and the lower organic phase containing the lipids was transferred to a fresh tube. Lipids were re-extracted from the remaining aqueous phase with 500 μL of ice cold chloroform. The two extracts were pooled and vacuum-dried. Dried lipid film was then reconstituted in chloroform: methanol 1:1 (v/v) prior to analysis by liquid chromatography-mass spectrometry (LC-MS).

Lipid extracts prepared from MVM-vesicles of normal and preeclamptic placentas were analyzed by LC-MS coupled to a Q-TOF detector (model micrOTOF Q II, Bruker) in negative mode as described by [28]. [M-H]-ions were extracted and integrated using the software Compass Data Analysis from Bruker.
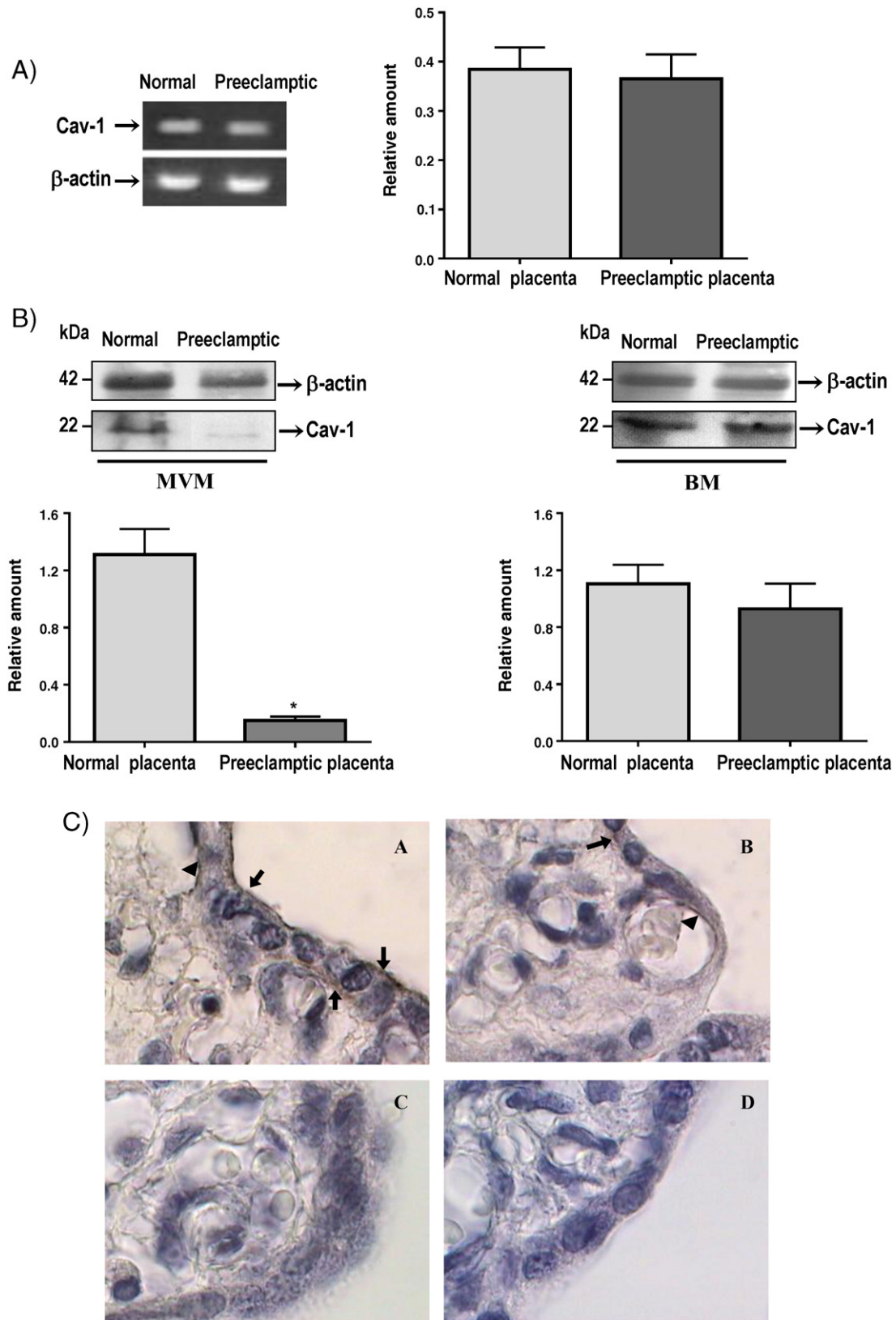
Fig. 1. Placental Cav-1 expression and localization in normal and preeclamptic placentas. A) Semiquantitative RT-PCR of Cav-1 gene expression in normal placenta and preeclamptic placenta. Densitometry analysis showed no significantly changes between normal and preeclamptic placentas. B) Representative Western blot for Cav-1 in normal and preeclamptic tissues. Densitometry of immunoblot showed a significantly decreased (*$P < 0.05$) in preeclamptic-MVM. However, no changes were observed in BM from normal and preeclamptic placentas. The relative values of Cav-1 were normalized against β-actin. Values are shown as mean ± SEM. Student's *t*-test was performed on the data, $n = 15$ in each experimental group. C) Immunolocalization of Cav-1 in representative sections of placental villous from normal and preeclamptic placentas. Arrows indicate Cav-1 labeling. In normal placentas Cav-1 was localized in the apical membrane of syncytiotrophoblast (arrows) and in endothelial cells (arrow heads) (panel A). In preeclamptic placentas, although Cav-1 was found in endothelial cells (arrow heads) and in the basal membrane (arrows) it was almost undetectable in the apical membrane of syncytiotrophoblast (panel B). Negative controls were performed by omitting the primary antibody and replaced by a non-immune rabbit serum (panel C and D). Magnification: 1000×.

2.9. Membrane order

A useful method to characterize the degree of order/mobility of the membrane lipids acyl chains is spin-label electron paramagnetic resonance (EPR) [29]. Adequate amount of 5-doxylstearic acid 1 mM was added to an aliquot (0.1 μmol phospholipid) of the vesicles in Tris–NaCl buffer pH 7.6, to achieve a 1:50 spin/phospholipid molar ratio. After 10 min incubation at room temperature (20 °C), 85 μL of potassium ferricyanide (200 mg/mL) was added to broaden the external spin label ESR signal. ESR spectra were recorded at 20 °C using an X-band ESR Spectrometer Bruker ECS 106 (Brucker Instruments, Inc., Berlin, Germany). The spectrometer settings were: center field 3485.00 G, sweep width 100.00 G, microwave power 20.0 mW, modulation frequency 50 KHz, modulation amplitude 0.203 G, conversion time 40.96 ms, time constant 655.36 ms, resolution 1024 points.

MVM and BM-vesicles order parameters (S) were calculated as described by Arvidson and co-workers [30]. Briefly, S is given by the ratio of the spectral anisotropy in the membranes ($A_{||} - A_{\perp}$) to the maximum anisotropy obtained in a rigidly oriented system (defined by A_{xx}, A_{yy}, A_{zz} the principal values of the spin label tensor) and was calculated from the respective ESR spectrum using the following equations:

$$S = \frac{(A_{||} - A_{\perp})}{A_{zz} - 0.5(A_{xx} - A_{yy})} \frac{\alpha'_0}{\alpha_0} \tag{1}$$

The A value was calculated using the following corrections expression:

$$A_{\perp} = A'_{\perp} + 1.4 \left\{ \frac{1 - (A_{||} - A'_{\perp})}{A_{zz} - 0.5(A_{xx} + A_{yy})} \right\} \quad (\text{for } A_{||} 0.45) \tag{2}$$

$A_{\perp}'$ and $A_{||}$ are the actual hyperfine constant values measured from the ESR spectrum. The polarity corrections term α'_0/α_0 is calculated by:

$$\alpha_0 = \frac{A_{||} = 2A_{\perp}}{3} \tag{3}$$

$$\alpha'_0 = \frac{A_{xx} + A_{yy} + A_{zz}}{3} \tag{4}$$

The S parameter gives a measure of the degree of structural order in the membrane, with parameters between $S = 1$ for a rapid spin-label motion about only one axis and $S = 0$ for a rapid isotropic motion. An increase in S parameter represents the consequence of an increase in the membrane order.

2.10. Statistical analysis

Statistical analysis of data was performed by GraphPad Prism v5 software (GraphPad Software, Inc. La Jolla, CA, USA). Results are given as mean ± S.E.M. Student's t-test was used to evaluate data statistically. A P-value of <0.05 was considered to be statistically significant.

3. Results

3.1. Expression of Cav-1 in preeclamptic placenta

First, we investigated the expression of Cav-1 at the transcriptional and protein levels. Total RNA was extracted and RT-PCR analysis was performed. An expected band of ~434-bp was obtained in normal and preeclamptic placentas and in both cases the semiquantitative PCR analysis showed no difference in Cav-1 expression (Fig. 1A). Instead, when the protein levels of Cav-1 was analyzed in MVM and BM of normal and preeclamptic term placentas by Western blot, some differences were found (Fig. 1B). In normal placentas the antibody revealed an

expected band of 22 kDa, in both fraction, MVM and BM. On the other hand, in preeclamptic placenta Cav-1 was principally found in BM. Semiquantitative analysis showed that Cav-1 decreased 6.5-fold in MVM of preeclamptic placentas, but the amount of Cav-1 in BM was similar compared to normal placenta.

No bands were observed when the primary antibody was omitted or when the Cav-1 antibody was preadsorbed with the Cav-1 specific peptide (data not shown).

In order to corroborate the results found by Western blot, chorionic villi from normal and preeclamptic placentas were analyzed by immunohistochemistry. In normal placentas Cav-1 was localized in the MVM of syncytiotrophoblast and in endothelial cells (Fig. 1C, panel A). Instead, in preeclamptic placentas, although Cav-1 was found in endothelial cells, nevertheless it was almost undetectable in the apical membrane of syncytiotrophoblast (Fig. 1C, panel B). Control sections treated with non-immune serum showed absence of labeling in normal and preeclamptic placentas as shown in Fig. 1C, panels C and D, respectively.

3.2. Expression of Cav-1 in DRMs

Considering that Cav-1 is localized mainly in membrane microdomains enriched in sphingolipids and cholesterol [13–16] we investigated the presence of this protein in DRMs fraction of both normal and preeclamptic placenta. Anyway, it is important to remember that the terms "membrane microdomains" and "DRMs" should not be used as synonyms because they have different origins and conceptual meanings [25]. However, a very much used approach in the current literature to investigate the interaction between a protein and membrane microdomains is the DRM technique. This technique takes profit from the selective solubilization of different lipids occurring when a biomembrane is submitted to the action of a nonionic detergent such as Triton X-100. Fig. 2 shows the immunoblot analysis of the fractions obtained by sucrose gradient ultracentrifugation as described under "Material and methods." As expected for polarized cells higher concentration of Cav-1 seems to be in MVM. In MVM of normal placentas it is distributed in light sucrose gradient fraction (1,2,3,4 and 5), being more concentrated
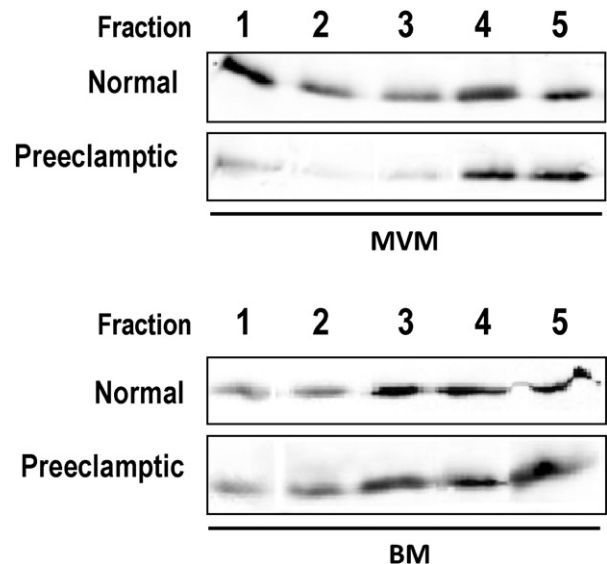
Fig. 2. Differential distribution of Cav-1 in sucrose gradient fraction of MVM and BM from normal and preeclamptic placentas. Detergent-resistant microdomains (DRMs) were isolated on a discontinuous sucrose gradient. In MVM of normal placentas, Cav-1 was concentrated at fraction 1, but in preeclamptic placentas, it is clearly diminished in fraction 1 and absent in fraction 2. Regarding BM, Cav-1 was preferentially found in the bottom of the sucrose gradient (fractions 3, 4 and 5) in both, normal and preeclamptic placentas.

at fraction 1, but in preeclamptic placentas it is mainly concentrated in fractions 4 and 5 while it is absent in fraction 2. On the other hand, Cav-1 is preferentially found in the bottom of the sucrose gradient in BM of normal and preeclamptic placenta (fractions 3, 4 and 5).
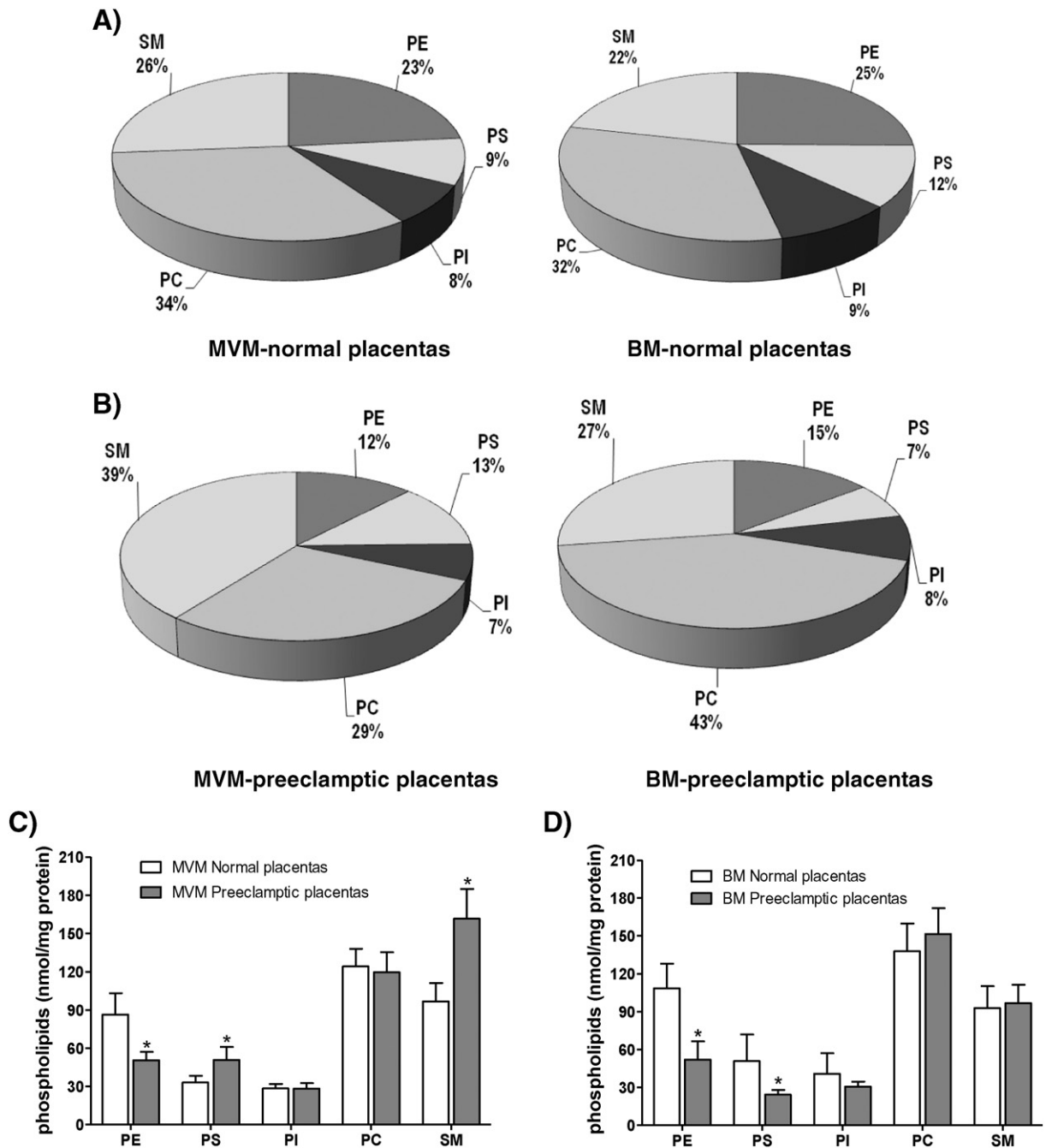
3.3. Membrane lipid composition

In order to explain the different localization of Cav-1 in chorionic villi from preeclamptic placenta compared to normal ones, we analyzed the lipid composition of MVM and BM-vesicles.

3.3.1. Phospolipid composition

The phospholipid composition was evaluated in MVM and BM-vesicles of human normal placenta. We found that the major phospholipid class was Phosphatidylcholine (PC) in both, MVM and BM. The relative amount of Phosphatidylserine (PS), Phosphatidylinositol (PI), Phosphatidylethanolamine (PE) and Sphingomyelin (SM) were similar in both membranes (Fig. 3A). Unexpectedly, in MVM of preeclamptic placentas we found that SM was the major phospholipid class (Fig. 3B).

On the other hand, when we analyzed the MVM phospholipid composition from preeclamptic placentas, we observed an increase of

Fig. 3. Phospholipid composition of plasma membrane from normal and preeclamptic placentas. A) Major phospholipid classes in MVM and BM-vesicles from normal placentas: Phosphatidylcholine (PC), Phosphatidylinositol (PI), Phosphatidylserine (PS), Phosphatidylethanolamine (PE) and Sphingomyelin (SM). Data are expressed as percentage of each phospholipid class respect to total phospholipids. B) Major phospholipid classes in MVM and BM-vesicles from preeclamptic placentas. Data are expressed as percentage of each phospholipid class respect to total phospholipids. C) Comparative phospholipid classes of MVM-vesicles from normal and preeclamptic placentas. D) Comparative phospholipid classes of BM-vesicles from normal and preeclamptic placentas. Data are expressed as nmoles of each phospholipid class per mg of protein. Values are shown as mean ± SEM. Student's t-test was performed on the data, $n = 20$ in each experimental group. (*$P < 0.05$).

Table 2

Cho/phospholipid and SM/PC molar ratios.

MVM-vesicles from preeclamptic placentas have an increase of SM content compared to normal ones without changes in Cho amount. Thus, we observed a significant increase of SM/PC ratio compared to normal ones ($n = 15$; *$P < 0.05$) and no change in the Cho/phospholipid ratio ($n = 27$).
No differences were observed either in SM/PC neither Cho/phospholipid ratios between BM-vesicles form normal and preeclamptic placentas.

	Cholesterol (nmol/mg of protein)	Total phospholipid (nmol/mg of protein)	Cho/total phospholipid
MVM normal placenta	308 ± 64	368.8 ± 53.7	0.84
MVM preeclamptic placenta	341 ± 63	411.1 ± 60.8	0.83
BM normal placenta	313 ± 38	430.8 ± 96.3	0.73
BM preeclamptic placenta	270 ± 29	355.2 ± 56.8	0.76
	PC (nmol/mg of protein)	SM (nmol/mg of protein)	SM/PC
MVM normal placenta	124 ± 14	97 ± 14	0.78
MVM preeclamptic placenta	120 ± 16	162 ± 23	1.35*
BM normal placenta	138 ± 22	93 ± 17	0.67
BM preeclamptic placenta	152 ± 20	97 ± 15	0.64

* $P < 0.05$, $n = 15$.

1.5-fold in the content SM and PS compared to normal ones (Fig. 3C). However, the relative amount of PE was significantly lower. Regarding phospholipid composition of BM from preeclamptic placentas, PE and PS were significantly decreased compared to normal placentas (Fig. 3D).

3.3.2. Cholesterol (Cho) content

We determined the content of Cho in MVM and BM from normal and preeclamptic placenta. We found no significant differences between BM and MVM from normal placentas. The same results were obtained for preeclamptic placentas. No changes were observed in Cho content when normal and preeclamptic placentas were compared (Table 2).

3.3.3. Fatty acid composition of amide-linked substituents to sphingomyelin in MVM vesicles obtained from preeclamptic and normal placentas

Since nature of the fatty acid moiety of the SM drastically affects membrane structure [30], we studied the SM species by LC-MS. Fig. 4A showed molecular species of SM of MVM-vesicles from normal and pre-eclamptic placentas. Mass spectrometry analysis allowed the determination of the total number of carbon atoms and double bonds in the fatty acid moiety for lipid classes. In all SM species, C18:1 sphingosine was the sphingoid base. The major SM molecular species in both normal and preeclamptic MVM-vesicles was 16:0 SM (42 and 41%, respectively), followed by 18:0 (25 and 19%, respectively). Interestingly, 18:1 SM content increased twenty five fold in MVM-vesicles from preeclamptic placentas compared to MVM-vesicles from normal ones (Fig. 4B). This result demonstrates that the increment of total SM observed in MVM from preeclamptic vesicles over normal one (Fig. 3) is exclusively due to the increment in the 18:1 SM specie.

3.4. Membrane order

SM is, together with Cho, relevant in determining lipid conformational order and packing [31–33].

As we mentioned above, MVM-vesicles from preeclamptic placentas have an increase of SM content compared to normal ones without changes in Cho amount. Thus, we only observed a significant increase of SM/PC ratio compared to normal ones ($n = 15$; $P < 0.05$) (Table 2). Accordingly with SM/PC ratio, the S parameter was significantly higher in MVM-vesicles from preeclamptic placentas comparing to normal ones, reflecting an increment reduction in membrane order (Fig. 5A).

No differences were observed either in SM/PC and Cho/total phospholipid ratios (Table 2) neither in the S parameter between BM-vesicles form normal and preeclamptic placentas (Fig. 5B).

4. Discussion

Fusion of placental villous cytotrophoblasts with the overlying syncytiotrophoblast is essential for the maintenance of successful pregnancy, and disturbances in this process have been implicated in

pathological conditions such as preeclampsia, a pregnancy disorder characterized by hypertension and proteinuria.

Results obtained in the present study demonstrated that Cav-1 protein expression was barely detectable in the apical membrane of syncytiotrophoblast from preeclamptic placentas. However, no change was observed at transcriptional levels. Even more, we observed a normal expression and localization in the basal membrane and
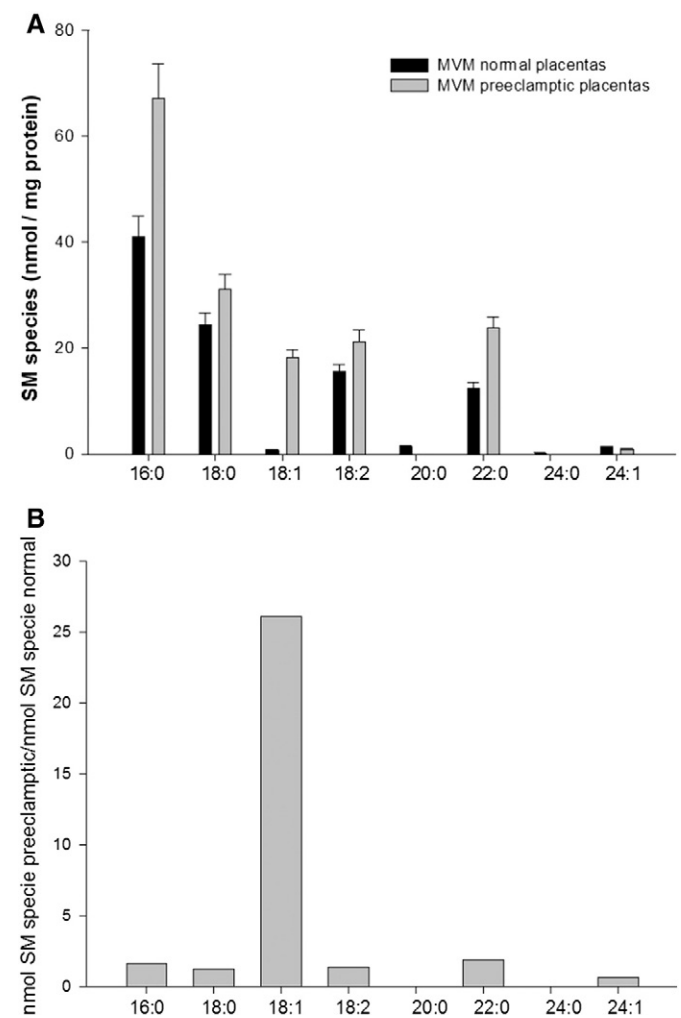
Fig. 4. Study of SM species in normal and preeclamptic MVM-vesicles by liquid chromatography-mass spectrometry (LC-MS). A) The major SM molecular species in both normal and preeclamptic MVM-vesicles. B) The relative increment of each SM species in MVM preeclamptic placentas over normal ones.

endothelium, suggesting a failure of Cav-1 insertion in the apical membrane of syncytiotrophoblast from preeclamptic placentas. Moreover, the presence of Cav-1 in DRMs of apical membranes of preeclamptic placentas was diminished, suggesting a deregulation in caveolas assembly. Caveolin itself is highly enriched in DRMs, indeed it is widely used as a raft marker, though it likely defines a subset of raft domains involved in caveolin-mediated traffic. Importantly, caveolin only associates with raft after its oligomerization; process which is stabilized by raft lipids present in plasma membrane and the late Golgi [34,35]. Specifically, the assembly of caveolas is dependent on the cooperative action of cavin and caveolin that bends the membrane and stabilizes the characteristic morphology of caveolas. The importance of Cho binding to caveolins to form caveolas is also established [36,37]. In addition, the most abundant negatively charged phospholipids of the plasma membrane, PS and the phosphoinositide phosphatidylinositol (4.5)-bisphosphate have been suggested to be concentrated in caveolas, forming physiologically distinct lipid pools [38–40]. These data suggest a major role of lipids in the regulation of the biophysical properties of the lipid bilayers, allowing an adequate formation and stabilization of caveolas.

On the other hand, it was postulated that the sphingolipid-rich apical domains are originated from sphingolipid- and cholesterol-enriched microdomains in trans-Golgi membranes [41–43]. These would then act as a sorting device for the delivery of apically directed cell surface components in polarized epithelial cells. Actually, it was reported that

changes in lipid composition such as the replacement of long-chain SM by short-chain SM, locally prevents the formation of a raft like liquid-ordered domain in the Golgi membranes which, in turn, could affect the generation of transport carriers or their fusion with target membranes [44].

Therefore, we analyzed the lipid membrane composition of normal and preeclamptic syncytiotrophoblast and found a different pattern of lipids in MVM and BM. Many authors have studied the phospholipid composition of syncytiotrophoblast cells but they did not distinguish between both membranes [4,5,45]. As syncytiotrophoblast is a polarized cell, the contribution of each phospholipid species is crucial to determine the apical or basal membrane transport function.

As it was expected, the more abundant phospholipid in normal membranes was PC, for both MVM and BM-vesicles. Instead, SM was the major phospholipid in MVM of preeclamptic placentas. Taking into account that SM/PC ratio determines the lipid order of the membrane [33], this increment in SM may alter this order. In addition, an increase in PS content was also observed in MVM from preeclamptic placentas. These findings correlate with previous results published by Baig et al. where they also found an increment of SM and PS in vesicles derived from MVM of preeclamptic placentas, which are shed into maternal circulation [5]. In total syncytiotrophoblast membranes from preeclamtic placentas, Huang and coworkers have also observed an increase in PS + PI content [45].
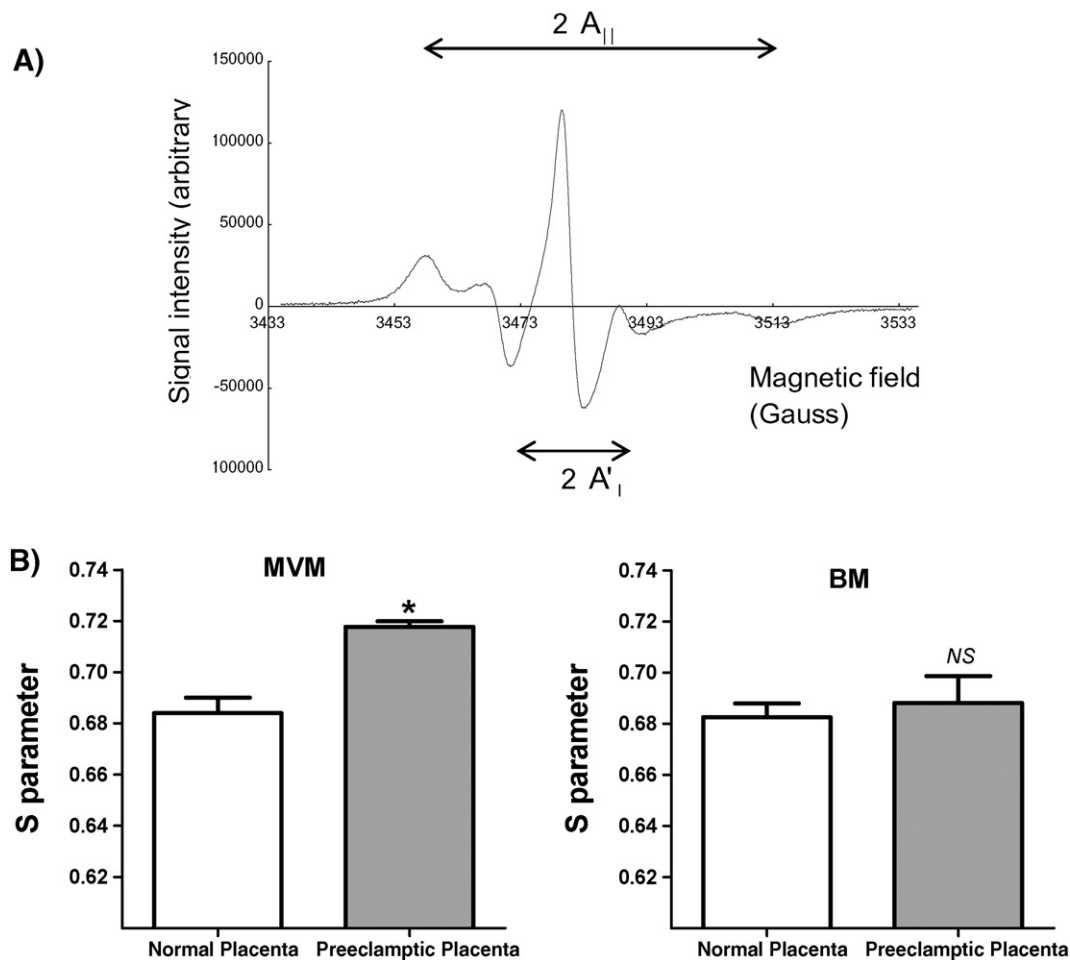
Fig. 5. Membrane order by Electron Spin Resonance (ESR). A) Representative ESR spectrum of the 5-doxilstearic acid inserted into the MVM from normal placentas. Vesicles were incubated with 5-doxylstearic acid (1:50 spin:phospholipid molar ratio) for 10 min at 20 °C and then, the ESR spectrum was obtain at 20 °C using an X-band ESR Spectrometer Bruker ECS 106. Membrane order was estimated from the spectrum by the order parameter S, using the equations written in Materials and methods. $A_{\parallel}$ and $A'_{\perp}$ values are the outer and inner extremes used in the calculation of the order parameter S. B) S parameter of MVM and BM from preeclamptic and normal placentas. Values are shown as mean ± SEM. Student's t-test was performed on the data, $n = 12$ in each experimental group. (*$P < 0.05$).

Furthermore, we also found a decrease in PE content in both membranes, MVM and BM, from preeclamptic placentas. As we previously reported, we proposed that this reduction might be due to an increment in the arachidonoyl phosphatidylethanolamine phopholipase D, enzyme that synthesizes anandamide by cleavage of PE from the membrane [46].

Regarding Cho, our data differ from those reported by Powell and co-workers [47]. They found that Cho content of syncytiotrophoblast-BM was lower than in MVM. However, our findings showed that Cho does not change significantly in both membranes. A possible explanation for these discrepancies could be the differences among the studied populations, in particular maternal nutritional status and ethnicity. Even more, some previous studies have reported that the lipid profile of human placenta may be modified by maternal nutrition [48].

In addition, we found that Cho content of preeclamptic-MVM was similar to that of normal placentas, a fact that could explain the observed normal expression of Cav-1 mRNA, considering that Cho regulates Cav-1 expression at the transcriptional level [49,50]. Pol et al. have added a level of complexity on this regulation showing that free cholesterol also regulates the traffic of newly synthesized protein through the Golgi complex to the plasma membranes, independent of caveolin synthesis [34].

It is well-known that the preferential interaction between SM and Cho in both, cell and model membranes, is a key factor in the formation of Cho- and SM- rich domains in membranes [41,51–52]. Cho and SM have both hydrogen-bond donor and acceptor groups that together with the Cho flat and extended hydrophobic structure promote the tight packing of SM and Cho into the liquid-ordered arrangement [53]. Thus, SM and Cho, are relevant in determining lipid conformational order and packing [31–33]. In this context, in a previous report we demonstrated that independently of the Cho content, SM/PC ratio determines the lipid order of the membrane; as the SM/PC ratio increase, the order of the membrane also increase [33]. In the present paper, membrane order was determined by EPR in normal and preeclamptic-MVM vesicles. We found differences, possibly related to the different SM content found between them, which may be affecting the localization of Cav-1 into sucrose fractions.

In agreement with Epand et al. [54], we also previously showed that when an unsaturated sphingolipid, oleoyl-SM or nervonoyl-SM, is included in a lipid mixture, no lateral phase separation is detected in fluid membranes containing Cho and DOPC (dioleylphophatidylcholine) [33]. Taking into account all these results, we suggest that the increment of SM, specifically the SM 18:1, in preeclamptic-MVM is directly related with the increment of the lipid order and the destabilization of caveolae.

In view of all these results, we propose that the altered lipid composition of preeclamptic MVM-vesicles may compromise cellular processes that critically depend on membrane structure, such as trafficking and sorting needed for normal caveolas assembling and, ultimately, the localization of Cav-1 into apical membranes. Anyway, we cannot rule out that lipid composition of preeclamptic Golgi may be affected which, in turn, could affect membrane structure and/or localization of proteins that are required for transport carrier biogenesis. This interesting issue will be the focus of further investigations.

In conclusion, we speculate that the increase of long and unsaturated SM molecular specie found in MVM-vesicles from preeclamptic placentas may disrupt the ability of SM to assemble into lipid rafts in the luminal leaflet of the bilayer, creating an unfavorable environment for appropriated location of Cav-1. Considering the important role Cav-1 has in biological processes, our findings open a new insight in the study of preeclampsia.

Declaration of interest

The author declares that there is no conflict of interest that would prejudice the impartiality of this scientific work.

Transparency document

The Transparency document associated with this article can be found, in online version.

References

[1] L. Ji, J. Brkić, M. Liu, G. Fu, C. Peng, Y.L. Wang, Placental trophoblast cell differentiation: physiological regulation and pathological relevance to preeclampsia, Mol. Asp. Med. 34 (2013) 981–1023.

[2] P.K. Ghosh, M. Mukherjea, Increase in fluidity of human placental syncytiotrophoblastic brush-border membrane with advancement of gestational age: a fluorescence polarization study, Biochim. Biophys. Acta 1236 (1995) 317–322.

[3] A. Sen, P.K. Ghosh, M. Mukherjea, Changes in lipid composition and fluidity of human placental basal membrane and modulation of bilayer protein functions with progress of gestation, Mol. Cell. Biochem. 187 (1998) 183–190.

[4] H.A. Korkes, N. Sass, A.F. Moron, N.O. Câmara, T. Bonetti, A.S. Cerdeira, I.D. Da Silva, L. De Oliveira, Lipidomic assessment of plasma and placenta of women with early-onset preeclampsia, PLoS One 9 (2014), e110747.

[5] S. Baig, J.Y. Lim, A.Z. Fernandis, M.R. Wenk, A. Kale, L.L. Su, A. Biswas, S. Vasoo, G. Shui, M. Choolani, Lipidomic analysis of human placental syncytiotrophoblast microvesicles in adverse pregnancy outcomes, Placenta 34 (2013) 436–442.

[6] A.E. Damiano, E. Zotta, C. Ibarra, Functional and molecular expression of AQP9 channel and UT-A transporter in normal and preeclamptic human placentas, Placenta 27 (2006) 1073–1081.

[7] M. Castro-Parodi, L. Levi, V. Dietrich, E. Zotta, A.E. Damiano, CFTR may modulate AQP9 functionality in preeclamptic placentas, Placenta 30 (2009) 642–648.

[8] S. del Monaco, Y. Assef, A. Damiano, E. Zotta, C. Ibarra, B.A. Kotsias, Characterization of the epithelial sodium channel in human pre-eclampsia syncytiotrophoblast, Medicina (B Aires) 66 (2006) 31–35.

[9] V. Dietrich, N. Szpilbarg, A.E. Damiano, Reduced expression of Na$^+$/H$^+$ exchanger isoform 3 (NHE-3) in preeclamptic placentas, Placenta 34 (2013) 828–830.

[10] R.W. Gross, X. Han, Lipidomics at the interface of structure and function in systems biology, Chem. Biol. 18 (2011) 284–291.

[11] M.P. Wymann, R. Schneiter, Lipid signalling in disease, Nat. Rev. Mol. Cell Biol. 9 (2008) 162–176.

[12] J.P. Slotte, Biological functions of sphingomyelins, Prog. Lipid Res. 52 (2013) 424–437.

[13] R.V. Stan, Structure of caveolae, Biochim. Biophys. Acta 1746 (2005) 334–348.

[14] R.G. Anderson, The caveolae membrane system, Annu. Rev. Biochem. 67 (1998) 199–225.

[15] R.R. Bruns, G.E. Palade, Studies on blood capillaries. General organization of blood capillaries in muscle, J. Cell Biol. 37 (1968) 244–276.

[16] T. Okamoto, A. Schlegel, P.E. Scherer, M.P. Lisanti, Caveolins, a family of scaffolding proteins for organizing "preassembled signaling complexes" at the plasma membrane, J. Biol. Chem. 273 (1998) 5419–5422.

[17] R.A. Zager, A. Johnson, S. Hanson, V. de la Rosa, Altered cholesterol localization and caveolin expression during the evolution of acute renal failure, Kidney Int. 61 (2002) 1674–1683.

[18] S. Byrne, A. Cheent, J. Dimond, G. Fisher, C.D. Ockleford, Immunocytochemical localization of a caveolin-1 isoform in human term extra-embryonic membranes using confocal laser scanning microscopy: implications for the complexity of the materno-fetal junction, Placenta 22 (2001) 499–510.

[19] T.W. Lyden, C.L. Anderson, J.M. Robinson, The endothelium but not the syncytiotrophoblast of human placenta expresses caveolae, Placenta 23 (2002) 640–652.

[20] E.A. Linton, B. Rodriguez-Linares, F. Rashid-Doubell, D.J. Ferguson, C.W. Redman, Caveolae and caveolin-1 in human term villous trophoblast, Placenta 24 (2003) 745–757.

[21] S. Byrne, J. Ahenkorah, B. Hottor, C. Lockwood, C.D. Ockleford, Immuno-electron microscopic localisation of caveolin 1 in human placenta, Immunobiology 212 (2007) 39–46.

[22] F. Rashid-Doubell, D. Tannetta, C.W. Redman, I.L. Sargent, C.A. Boyd, E.A. Linton, Caveolin-1 and lipid rafts in confluent BeWo trophoblasts: evidence for rock-1 association with caveolin-1, Placenta 28 (2007) 139–151.

[23] K. Smith-Jackson, M.R. Hentschke, C.E. Poli-de-Figueiredo, B.E. Pinheiro da Costa, L.O. Kurlak, F. Broughton Pipkin, A. Czajka, H.D. Mistry, Placental expression of eNOS, iNOS and the major protein components of caveolae in women with pre-eclampsia, Placenta 36 (2015) 607–610.

[24] A. Damiano, E. Zotta, J. Goldstein, I. Reisin, C. Ibarra, Water channel proteins AQP3 and AQP9 are present in syncytiotrophoblast of human term placenta, Placenta 22 (2001) 776–781.

[25] V. Herlax, S. Maté, O. Rimoldi, L. Bakas, Relevance of fatty acid covalently bound to *Escherichia coli* alpha-hemolysin and membrane microdomains in the oligomerization process, J. Biol. Chem. 284 (2009) 25199–25210.

[26] E.G. Bligh, W.J. Dyer, A rapid method of total lipid extraction and purification can, J. Biochem. Physiol. 37 (1959) 911–917.

[27] C.H. Fiske, Y.P. Subbarow, The colorimetric determination of phosphorus, J. Biol. Chem. 66 (1925) 375–400.

[28] A.H. Merrill Jr., M.C. Sullards, J.C. Allegood, S. Kelly, E. Wang, Sphingolipidomics: high-throughput, structure-speciWc, and quantitative analysis of sphingolipids by liquid chromatography tandem mass spectrometry, Methods 36 (2005) 207–224.

[29] D. Marsh, L.I. Horvath, Structure, dynamics and composition of the lipid–protein interface. Perspectives from spin labelling, Biochim. Biophys. Acta 1376 (1998) 267–296.

[30] G. Arvidson, G. Ronquist, G. Wikander, A.C. Ojteg, Human prostasome membranes exhibit very high cholesterol/phospholipid ratios yielding high molecular ordering, Biochim. Biophys. Acta 984 (1989) 167–173.

[31] K. Simons, W.L.C. Vaz, Model systems, lipid rafts, and cell membranes, Annu. Rev. Biophys. Biomol. Struct. 33 (2004) 269–295.

[32] P.M. Rodi, M.S. Cabeza, A.M. Gennaro, Detergent solubilization of bovine erythrocytes. Comparison between the insoluble material and the intact membrane, Biophys. Chem. 122 (2006) 114–122.

[33] S. Maté, J.V. Busto, A.B. García-Arribas, J. Sot, R. Vazquez, V. Herlax, C. Wolf, L. Bakás, F.M. Goñi, *N*-nervonoylsphingomyelin (C24:1) prevents lateral heterogeneity in cholesterol-containing membranes, Biophys. J. 106 (2014) 2606–2616.

[34] A. Pol, S. Martin, M.A. Fernandez, M. Ingelmo-Torres, C. Ferguson, C. Enrich, R.G. Parton, Cholesterol and fatty acids regulate dynamic caveolin trafficking through the Golgi complex and between the cell surface and lipid bodies, Mol. Biol. Cell 16 (2005) 2091–2105.

[35] S. Monier, D.J. Dietzen, W.R. Hastings, D.M. Lublin, T.V. Kurzchalia, Oligomerization of VIP21-caveolin in vitro is stabilized by long chain fatty acylation or cholesterol, FEBS Lett. 388 (1996) 143–149.

[36] M.R. Breen, M. Camps, F. Carvalho-Simoes, A. Zorzano, P.F. Pilch, Cholesterol depletion in adipocytes causes caveolae collapse concomitant with proteosomal degradation of cavin-2 in a switch-like fashion, PLoS One 7 (2012), e34516.

[37] M. Murata, J. Peränen, R. Schreiner, F. Wieland, T.V. Kurzchalia, K. Simons, VIP21/caveolin is a cholesterol-binding protein, Proc. Natl. Acad. Sci. U. S. A. 92 (1995) 10339–10343.

[38] G.D. Fairn, N.L. Schieber, N. Ariotti, S. Murphy, L. Kuerschner, R.I. Webb, S. Grinstein, R.G. Parton, High-resolution mapping reveals topologically distinct cellular pools of phosphatidylserine, J. Cell Biol. 194 (2011) 257–275.

[39] A. Fujita, J. Cheng, K. Tauchi-Sato, T. Takenawa, T. Fujimoto, A distinct pool of phosphatidylinositol 4.5-bisphosphate in caveolae revealed by a nanoscale labeling technique, Proc. Natl. Acad. Sci. U. S. A. 106 (2009) 9256–9561.

[40] L.J. Pike, L. Casey, Localization and turnover of phosphatidylinositol 4.5-bisphosphate in caveolin-enriched membrane domains, J. Biol. Chem. 271 (1996) 26453–26456.

[41] K. Simons, E. Ikonen, Functional rafts in cell membranes, Nature 387 (1997) 569–572.

[42] K. Simons, G. van Meer, Lipid sorting in epithelial cells, Biochemistry 27 (1988) 6197–6202.

[43] G. Van Meer, E.H.K. Stelzer, R.W. Wijnaendts-van-Resandt, K. Simons, Sorting of sphingolipids in epithelial (Madin-Darby canine kidney) cells, J. Cell Biol. 105 (1987) 1623–1635.

[44] J.C. Holthuis, T. Pomorski, R.J. Raggers, H. Sprong, G. Van Meer, The organizing potential of sphingolipids in intracellular membrane transport, Physiol. Rev. 81 (2001) 1689–1723.

[45] X. Huang, A. Jain, M. Baumann, M. Körner, D. Surbek, P. Bütikofer, C. Albrecht, Increased placental phospholipid levels in pre-eclamptic pregnancies, Int. J. Mol. Sci. 14 (2013) 3487–3499.

[46] C. Abán, G.F. Leguizamón, M. Cella, A. Damiano, A.M. Franchi, M.G. Farina, Differential expression of endocannabinoid system in normal and preeclamptic placentas: effects on nitric oxide synthesis, Placenta 34 (2013) 67–74.

[47] T.L. Powell, T. Jansson, N.P. Illsley, M. Wennergren, M. Korotkova, B. Strandvik, Composition and permeability of syncytiotrophoblast plasma membranes in pregnancies complicated by intrauterine growth restriction, Biochim. Biophys. Acta 1420 (1999) 86–94.

[48] J. Araya, C. Soto, A.M. Aguilera, C. Bosco, R. Monlina, Modification of the lipid profile of human placenta by moderate maternal undernutrition, Rev. Med. Chil. 122 (5) (1995) 503–509.

[49] D. Hailstones, L.S. Sleer, R.G. Parton, K.K. Stanley, Regulation of caveolin and caveolae by cholesterol in MDCK cells, J. Lipid Res. 39 (1998) 369–379.

[50] C.J. Fielding, A. Bist, P.E. Fielding, Caveolin mRNA levels are up-regulated by free cholesterol and down-regulated by oxysterols in fibroblast monolayers, Proc. Natl. Acad. Sci. U. S. A. 94 (1997) 3753–3758.

[51] T.K.M. Nyholm, D. Lindroos, J.P. Slotte, Construction of a DOPC/PSM/cholesterol phase diagram based on the fluorescence properties of *trans*-parinaric acid, Langmuir 27 (2011) 8339–8350.

[52] M. Lonnfors, J.P. Doux, J.P. Slotte, Sterols have higher affinity for sphingomyelin than for phosphatidylcholine bilayers even at equal acyl-chain order, Biophys. J. 100 (2011) 2633–2641.

[53] P.J. Quinn, C. Wolf, Thermotropic and structural evaluation of the interaction of natural sphingomyelins with cholesterol, Biochim. Biophys. Acta 1788 (2009) 1877–1889.

[54] R.M. Epand, R.F. Epand, Non-raft forming sphingomyelin cholesterol mixtures, Chem. Phys. Lipids 132 (2004) 37–46.